ACS Macro Letters

Letter

pubs.acs.org/macroletters

Controlling the Location of Nanoparticles in Colloidal Assemblies of Amphiphilic Polymers by Tuning Nanoparticle Surface Chemistry

Qingjie Luo, Robert J. Hickey, and So-Jung Park*

Department of Chemistry, University of Pennsylvania, 231 South 34th Street, Philadelphia, Pennsylvania 19104, United States

Supporting Information

ABSTRACT: Here, we report a simple method to control the location of nanoparticles in colloidal block-copolymer assemblies by using nanoparticles modified with mixed surface ligands. The binary self-assembly of amphiphilic polymers of polystyrene-*b*-poly(acrylic acid) (PS-*b*-PAA) and gold nanoparticles (AuNPs) modified with a hydrophobic ligand, dodecanethiol (DT), led to polymer micelles with nanoparticles segregated in the core of polymer micelles. On the other hand, AuNPs modified with mixed ligands of mercaptoundecanol (MUL) and DT were distributed at the PS−PAA interface, reducing the interfacial energy between the two polymers. This result was in good agreement with the prediction by the surface energy calculations. We also showed that the AuNPs with mixed ligands can decorate preformed polymer assemblies by the interfacial self-assembly. Furthermore, we demonstrated the compartmentalization of two different types of nanoparticles in colloidal polymer assemblies based on the strategy.

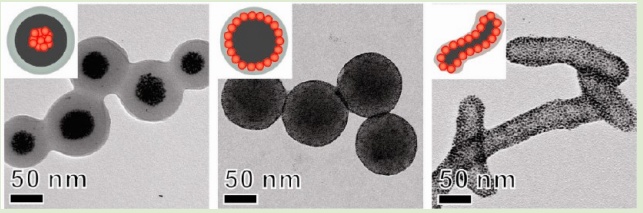

Colloidal self-assembly of amphiphilic block-copolymers and inorganic nanoparticles offers a way to create solution processable functional materials with useful chemical and mechanical properties of polymers and the unique size-dependent properties of nanoparticles for various applications including medical imaging and drug delivery.[1−4] Because the distribution of nanoparticles in the polymer matrixes is an important factor that determines the properties of such hybrid structures, it is of great interest to form polymer assemblies with controllable nanoparticle arrangements. A range of different types of nanoparticles (e.g., semiconducting,[5] magnetic,[6] and metallic nanoparticles[7]) have been encapsulated in various polymer assemblies. For example, Eisenberg and co-workers have demonstrated a strategy to incorporate polymer-grafted nanoparticles in the membrane of polymer vesicles.[8] Taton and co-workers have fabricated nanoparticle-loaded polymer micelles where alkyl-terminated nanoparticles were uniformly embedded in the hydrophobic polymer core.[9,10] Using a similar method, we have shown that the arrangement of nanoparticles and the polymer morphology can be controlled by changing the initial solvent composition, polymer lengths, and nanoparticle weight fractions.[11] Unique cavity-like assemblies of hydrophobic nanoparticles were formed in A−B polymer assemblies where nanoparticles were arranged at the B−B interface.[12−14] We have also prepared polymer vesicles densely packed with magnetic nanoparticles and showed that the spatial arrangement of nanoparticles in the polymer matrix significantly affects the magnetic relaxation rate of surrounding water.[11]

In this communication, we report a simple method to control the location of gold nanoparticles (AuNPs) in colloidal polymer assemblies by tuning the nature of the nanoparticle surface. For bulk and thin film composite systems, various factors affecting the binary self-assembly of block-copolymers and nanoparticles have been investigated including the size of the nanoparticles, the molecular weight of polymers, and the nanoparticle surface ligands.[15−17] For example, Kramer and co-workers have localized polymer-grafted AuNPs in different domains of lamellar assemblies of block-copolymers by changing the polymer composition grafted onto AuNPs.[18] Emrick and co-workers have shown that the location of nanoparticles in block-copolymer assemblies can be controlled by varying the ratio between hydrophobic and hydrophilic ligands on nanoparticles.[19] On the contrary, the ability to control the nanoparticle distribution in the solution-phase self-assembly is still quite limited. In this study, we show for the first time that the arrangement of nanoparticles in A−B polymer micelles can be controlled from the core of the polymer micelles to the A−B polymer interface by using mixed nanoparticle ligands. We also demonstrate that different types of nanoparticles can be compartmentalized in different locations of colloidal polymer assemblies using the approach.

In typical experiments, AuNPs stabilized with dodecanethiol (DT) were first synthesized by the Brust−Schiffrin method.[20] Then, a fraction of DT ligands of nanoparticles was replaced with 11-mercapto-1-undecanol (MUL) by the ligand exchange,[12,15] resulting in nanoparticles with mixed hydrophobic (DT) and hydrophilic (MUL) ligands (Figure S1, Supporting Information). The ratio of DT to MUL was controlled by varying the concentration of MUL in the solution used for the ligand exchange (Table S1, Supporting Information). The final

Received: November 13, 2012
Accepted: January 8, 2013
Published: January 11, 2013

   dx.doi.org/10.1021/mz3006044 | *ACS Macro Lett.* 2013, 2, 107−111

ratios of DT and MUL on nanoparticles were determined by ^{1}H NMR (Figure S2 and Table S1, Supporting Information). The synthesized nanoparticles were assembled with amphiphilic polymers of polystyrene and poly(acrylic acid) (PS-*b*-PAA) using the selective solvent method.[11] Briefly, AuNPs in chloroform or ethanol (1.7 μM, 50 μL) were mixed with PS_{250}-*b*-PAA_{14} dissolved in *N*,*N*-dimethylformamide (DMF) (4 μM, 500 μL). To induce self-assembly, 0.3 mL of purified water (17.9 MΩ) was slowly added to the mixture at the rate of 10 μL/30 s while stirring. The solution was then dialyzed against water for 24 h. In all experiments, the volume fraction of AuNPs over the combined volume of AuNPs and polymers was kept constant at 0.06. The resulting assemblies were characterized by transmission electron microscopy (TEM), scanning transmission electron microscopy (STEM), energy-dispersive X-ray spectroscopy (EDS), and dynamic light scattering (DLS).

Figure 1 presents TEM images of binary assemblies of PS-*b*-PAA and AuNPs with varying surface ligands. The AuNPs

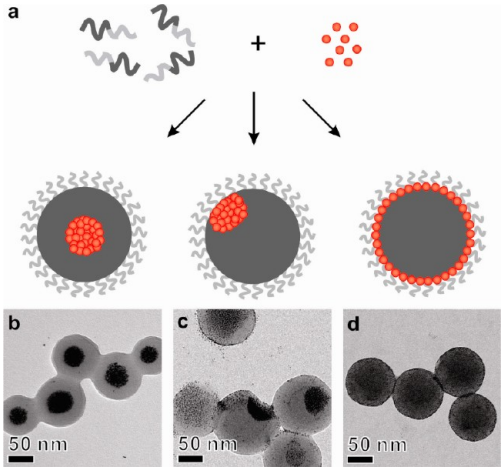

Figure 1. (a) Pictorial description of the self-assembly of PS_{250}-*b*-PAA_{14} and AuNPs with varying surface ligands. Light gray lines, dark gray lines, and red spheres represent PAA, PS, and AuNP, respectively. (b) A TEM image of coassemblies prepared with AuNPs modified with 100% DT. (c) A TEM image of coassemblies prepared with AuNPs modified with 75% DT and 25% MUL. (d) A TEM image of coassemblies prepared with AuNPs modified with 20% DT and 80% MUL. Note that the PAA layer is not visible in TEM images.

immobilized with 100% DT segregated into the PS core of polymer micelles due to the favorable enthalpic interaction between the hydrophobic nanoparticles and the PS block as well as the attractive interaction between AuNPs (Figure 1b). As the fraction of MUL increases to 25% or 33%, the nanoparticle aggregates moved toward the PS−PAA interface, forming Janus-type particles (Figure 1c). The asymmetric assembly formed at the MUL % range is reminiscent of the report by Chen and co-workers where single gold nanoparticles are eccentrically embedded in polymer micelles when nanoparticles and polymers are self-assembled in the presence of hydrophobic and hydrophilic thiols.[21] A further increase of the MUL % over 50 (50%, 60%, 80%, 100%) led to AuNPs distributed at the PS−PAA interface (Figure 1d). Note that TEM images are two-dimensional projections of three-dimensional objects. Therefore, the dark contrast at the edges of polymer assemblies indicates the selective accumulation of nanoparticles at the PS−PAA interface.

Understanding the wetting properties of nanoparticles and polymers is important for the rational design of polymer nanocomposites.[16,22,23] The spatial arrangements of nanoparticles with varying surface ligands in polymer assemblies can be explained by the interfacial energies between two polymer blocks, A and B, and nanoparticles. Nanoparticles can locate at the A−B interface of two polymers if the criterion of

$$|\sigma_{A/NP} - \sigma_{B/NP}| < \sigma_{A/B} \quad (1)$$

is satisfied, where $\sigma_{A/NP}$, $\sigma_{B/NP}$, and $\sigma_{A/B}$ are the interfacial energies of A−AuNP, B−AuNP, and A−B pairs, respectively.[16,23,24] The interfacial energy, $\sigma_{1/2}$, between two interacting components, 1 and 2, is defined as

$$\sigma_{1/2} = (\sqrt{\gamma_1} - \sqrt{\gamma_2})^2 \quad (2)$$

where γ is the surface energy.[25] The surface energy can be estimated by measuring contact angle, θ

$$\frac{\gamma_L}{\sqrt{\gamma_L^D}}(1 + \cos\theta) = 2\sqrt{\gamma_S^D} + 2\sqrt{\gamma_S^P}\sqrt{\frac{\gamma_L^P}{\gamma_L^D}} \quad (3)$$

where γ_L is the surface energy of liquids and γ_S is the surface energy of solids.[26] The γ_L^D and γ_S^D denote dispersion components, and γ_L^P and γ_S^P denote polar components. From contact angle measurements with a polar and a nonpolar liquid with known surface energies, γ_S^P and γ_S^D can be obtained from the slope and the intercept of eq 3.

We used these relationships to predict the molar ratio of MUL and DT that induces the interfacial assembly of AuNPs. To estimate the interfacial energies between modified AuNPs and two polymer blocks, PS and PAA, gold thin films coated with DT and MUL were used as model systems for ligand-modified AuNPs. Water and formamide were used as test solvents for contact angle measurements. The ligand-modified gold films were prepared by immersing freshly deposited gold films into ethanolic solutions of DT or DT/MUL mixtures (3 mM) for two days at room temperature. The surface energies of modified Au films were estimated from the contact angle measurements for varying molar ratios of DT and MUL. As expected, the surface energy gradually increased as the percentage of MUL increased (Figure S4, Supporting Information), which is consistent with previous reports.[27,28] The $\sigma_{PS/NP}$ and $\sigma_{PAA/NP}$ values were then calculated from the surface energies using eq 2. As plotted in Figure 2, the $|\sigma_{PS/NP} - \sigma_{PAA/NP}|$ value decreases with increasing MUL percentage (Figure 2) and becomes smaller than $\sigma_{PS/PAA}$ (3.43 mJ/m^2) at

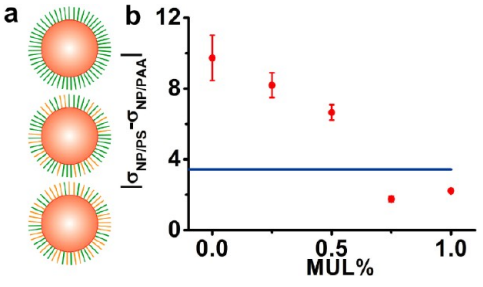

Figure 2. (a) Pictorial description of nanoparticles modified with two different ligands at different ratios. Green lines and orange lines represent two different ligands. (b) The $|\sigma_{PS/NP} - \sigma_{PAA/NP}|$ values at varying MUL % on nanoparticle surfaces. The blue line indicates the interfacial energy between PS and PAA.

dx.doi.org/10.1021/mz3006044 | *ACS Macro Lett.* 2013, 2, 107−111

about 61% MUL (Supporting Information). Eventually, the $\sigma_{PS/NP} - \sigma_{PAA/NP}$ becomes negative for 100% MUL, and the absolute value of $|\sigma_{PS/NP} - \sigma_{PAA/NP}|$ becomes closer to $\sigma_{PS/PAA}$. Therefore, the minimum value of $|\sigma_{PS/NP} - \sigma_{PAA/NP}|$ is found at an MUL % between 65% and 100%. These data indicate that NPs with MUL % larger than 65% can reside at the PS–PAA interface, reducing the interfacial energy between PS and PAA. It also indicates that the ideal MUL % for interfacial assembly should be larger than 65% and smaller than 100%.

This prediction is in a good agreement with the experimental data presented in Figure 1. Among four different MUL % (50%, 60%, 80%, 100%) that showed the interfacial assembly, the nanoparticle distribution was most even at 80% MUL (Figure 1d and Figure S6, Supporting Information). This result is consistent with the prediction that the most effective MUL % for reducing the PS–PAA interfacial energy is in between 65% and 100% (Figure 2). However, it is worth noting that the interfacial assembly of nanoparticles was found over a wider range of MUL % than predicted. This is partly due to the fact that the surface energy of modified AuNPs can be different from that of modified gold films, as reported by Stellacci and co-workers.[27] Moreover, the two ligands on AuNPs can phase-segregate to maximize the interaction between PS and DT and the interaction between PAA and MUL rather than forming homogeneously mixed monolayers. Also, note that the prediction by the interfacial energy calculation does not consider the distribution in ligand compositions, while the actual ligand composition is distributed about the measured average values with fractions of nanoparticles with more or less MUL % than the average value. Nonetheless, the interfacial energy calculation presented in Figure 2 provides a useful guidance for the solution-phase interfacial assemblies of nanoparticles and amphiphilic polymers.

The EDS measurements were consistent with the TEM observations (Figure 3). The Au intensity profile of the assemblies formed with 100% DT showed a Gaussian-shape curve indicating that AuNPs concentrated in the center of polymer micelles (Figure 3a). The assemblies with 80% MUL, on the other hand, showed high intensities at the edges of the micelle, confirming the assembly of nanoparticles at the PS–PAA interface (Figure 3b). On the basis of the size of the assemblies (Figure 3c,d), it is likely that the assemblies formed at 80% MUL adopt the compound micelle structure,[29,30] which is composed of a micelle containing reverse micelles in the core. Because varying numbers of reverse micelles can be incorporated in compound micelles, they typically show broad size distributions.[29] However, the interfacial assemblies prepared with 80% MUL AuNPs were fairly uniform and showed a narrow size distribution with the standard deviation of 8% from TEM measurements (Figure 3d). This result indicates that the incorporation of amphiphilic AuNPs regulates the characteristic length scale and overall size of polymer assemblies, as shown for polymer melts and larger colloidal polymer particles.[31] It is interesting to note that the size distribution becomes broader when the MUL % was increased to 100% or decreased to 50% (Figure 3e). For 100% MUL, polymer assemblies might be preformed before nanoparticles start associating with polymers at the PS–PAA interface or in the PAA block because of the hydrophilic nature of the NPs, resulting in a broader size distribution.

The result of 100% MUL suggests that nanoparticle-decorated polymer assemblies can be prepared from preformed polymer assemblies (Figure 4). This approach provides a

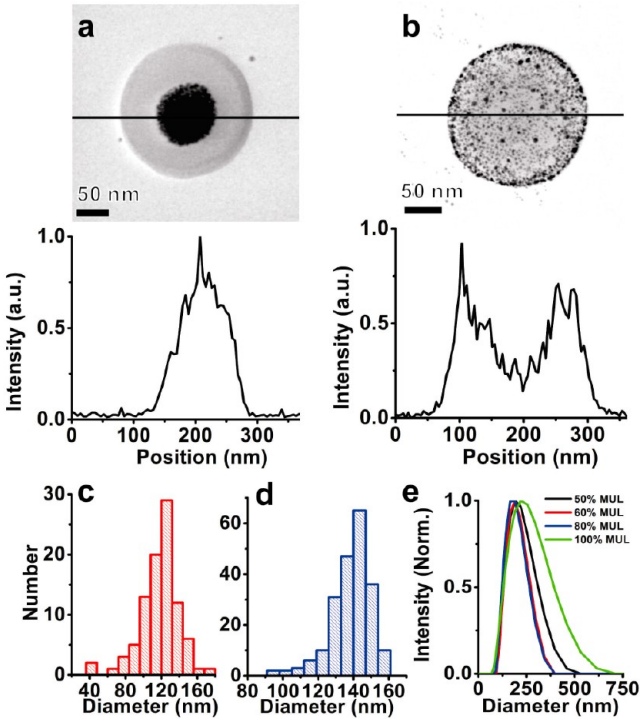

Figure 3. (a,b) STEM images and EDS line scans of the assemblies prepared with 100% DT (a) and 80% MUL (b). The EDS line profile (gold L_α line) is an average of multiple scans. (c,d) Size distribution histograms of the assemblies prepared with 100% DT (c) and the assemblies prepared with 80% MUL (d) obtained from TEM images. (e) DLS data for assemblies prepared with 50%, 60%, 80%, and 100% MUL.

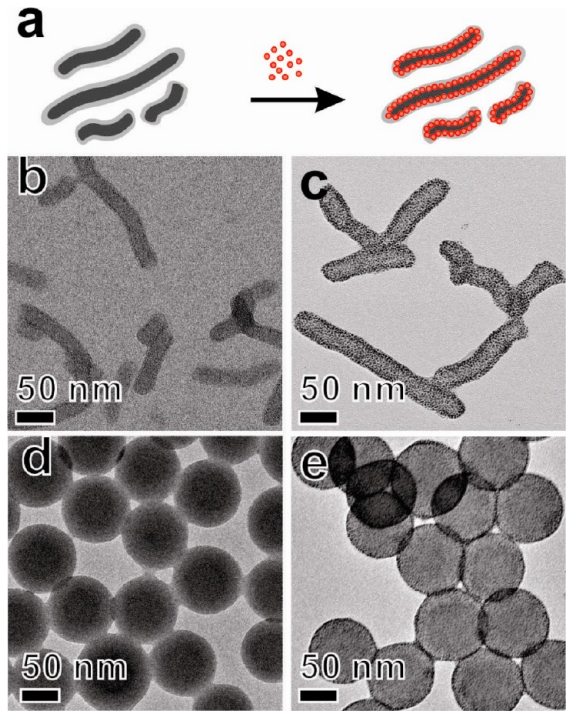

Figure 4. (a) Schematic description for the formation of rod-like micelles decorated with AuNPs. (b,c) Rod-like micelles of PAA_{96}–PS_{48} (b) before and (c) after the nanoparticle assembly. (d,e) Commercial carboxylic acid terminated polystyrene beads (100 nm) (d) before and (e) after the nanoparticle assembly.

dx.doi.org/10.1021/mz3006044 | ACS Macro Lett. 2013, 2, 107–111

simple way to decorate various types of polymeric nanostructures with inorganic nanoparticles and is particularly useful for nonspherical assemblies that are difficult to prepare using the simultaneous self-assembly of amphiphilic polymers and nanoparticles. To test the feasibility of the approach, rod-like micelles were first prepared by dispersing PS_{96}-*b*-PAA_{48} in water by sonication. An ethanol solution of AuNPs immobilized with 100% MUL (2.7 μM, 100 μL) was then slowly added to the aqueous solution of micelles (2 mg/mL, 15 μM, 10 μL) while stirring the solution. The self-assembly was induced by the slow water addition (1.8 mL) followed by dialysis. This procedure led to rod-like micelles densely coated with AuNPs, as revealed by TEM (Figure 4a,b). As another example, commercial carboxylic acid modified polystyrene beads were used for the interfacial assembly. As shown in Figure 4d, polystyrene beads uniformly coated with nanoparticles were formed by the same procedure.

With these capabilities, we fabricated multicomponent assemblies where gold and iron oxide nanoparticles are embedded in different locations of polymer assemblies (Figure 5). We have previously shown that iron oxide nanoparticles stabilized with oleic acids can form unique radial arrays at the PS−PS interface in compound micelles of PS-*b*-PAA (Figure 5b).[11,32] The ternary self-assembly of iron oxide nanoparticles, AuNPs (80% MUL or 100% MUL), and PS-*b*-PAA resulted in layered assemblies with AuNPs located at the PS−PAA interface and iron oxide nanoparticles located in between the polymer core and polymer shell[11] of compound micelles (Figure 5a,d). For a typical experiment, magnetic NPs were first mixed with PS_{144}-*b*-PAA_{49} (2 μM, 20 μL) in DMF and then mixed with AuNPs (4.7 μM, 10 μL) in ethanol, followed by the slow water addition and dialysis. The distance between two nanoparticle layers can be potentially controlled by varying the molecular weight of polymers or nanoparticle volume fractions.[13] The EDS data confirmed that iron oxide nanoparticles and AuNPs are arranged at two different radial positions of polymer assemblies (Figure 5d). The distribution of iron oxide nanoparticles can be controlled by using a different initial cosolvent for nanoparticles and polymers as we previously reported.[11] When THF was used instead of DMF, iron oxide nanoparticles are embedded throughout the PS matrix rather than forming shell-like assemblies as previously reported (Figure 5e).[10,11] Figure 5f presents the coassemblies of AuNPs and iron oxide nanoparticles prepared in the condition that favors the uniform distribution of iron oxide nanoparticles. It is apparent from TEM images and EDS line scans that iron oxide nanoparticles are embedded in the PS core, while AuNPs are located at the PS−PAA interface.

In summary, we demonstrated a strategy to control the location of nanoparticles in colloidal solution-phase assemblies of amphiphilic polymers. Depending on the ratio between hydrophobic and hydrophilic surface ligands, particles either localized at the interface between PS and PAA blocks or aggregated in the center of the assemblies. Uniform interfacial assemblies of AuNPs were obtained with AuNPs modified with 80% MUL and 20% DT, which is in good agreement with the prediction by interfacial energy calculations. Compared to the hollow nanoparticle capsules fabricated by the interfacial assembly at the oil/water interface of emersions,[33] the binary assembly of nanoparticles and polymers reported here results in more stable nanoparticle capsules supported by polymer templates. On the basis of the approach, we fabricated multifunctional assemblies where iron oxide nanoparticles and AuNPs are compartmentalized at different locations of polymer matrixes. Furthermore, we demonstrated that MUL-modified AuNPs can decorate preformed assemblies of amphiphilic polymers. This approach can be potentially useful for functionalizing polymer particles with targeting molecules or drugs for biomedical applications.

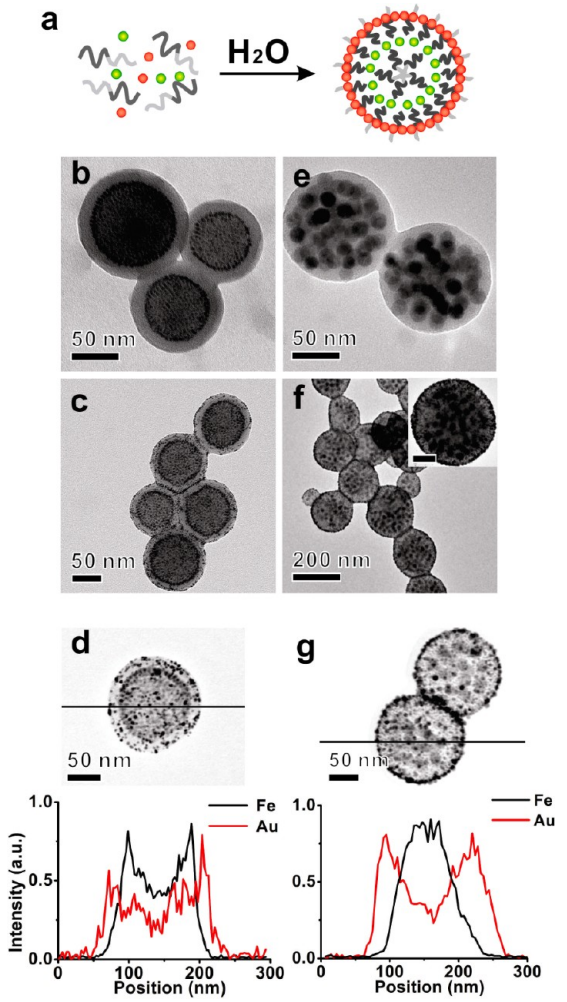

Figure 5. (a) Pictorial description for the formation of multicomponent layered assemblies of AuNPs and magnetic nanoparticles. Red dots and green dots represent AuNPs and iron oxide nanoparticles, respectively. (b) Compound micelles with 4.5 nm magnetic nanoparticles arranged in between the polymer core and polymer shell. (c) Compound micelles with 4.5 nm iron oxide nanoparticles arranged in between the polymer core and polymer shell and AuNPs (80% MUL) at the PS−PAA interface. (d) An STEM image and EDS Au intensity (L_α line) and Fe intensity (K_α line) profiles of the assemblies shown in (c). (e) Polymer micelles encapsulated with 15.7 nm magnetic nanoparticles in the PS domain. (f) Polymer micelles encapsulated with 15.7 nm magnetic nanoparticles in the PS domain and AuNPs (100% MUL) at the PS−PAA interface. The inset shows a higher magnification TEM image (scale bar: 50 nm). (g) An STEM image and the EDS Au intensity (L_α line) and Fe intensity (K_α line) profiles of the assemblies shown in (f).

■ ASSOCIATED CONTENT

Supporting Information

Detailed experimental procedures, TEM, UV−vis spectra, and ^{1}H NMR spectra of AuNPs, UV−vis spectra, additional TEM images of assemblies, and contact angle measurement data.

dx.doi.org/10.1021/mz3006044 | *ACS Macro Lett.* 2013, 2, 107−111

This material is available free of charge via the Internet at http://pubs.acs.org.

AUTHOR INFORMATION

Corresponding Author

*E-mail: sojungp@sas.upenn.edu.

Notes

The authors declare no competing financial interest.

ACKNOWLEDGMENTS

This work was supported by the NSF career award (DMR 0847646) and ARO young investigator award (W911NF-09-1-0146). The STEM and EDS measurements were carried out using instrumentation at Penn Regional Nanotechnology Facility. The authors thank Dr. Shu Yang and Dr. Yudi Rahmawan for their help with contact angle measurements. The authors thank Dr. Jie Zhang for his kind gift of block-copolymer (PS_{96}-*b*-PAA_{48}).

REFERENCES

(1) Gao, X.; Cui, Y.; Levenson, R. M.; Chung, L. W. K.; Nie, S. *Nat. Biotechnol.* **2004**, *22*, 969.
(2) Euliss, L. E.; Grancharov, S. G.; O'Brien, S.; Deming, T. J.; Stucky, G. D.; Murray, C. B.; Held, G. A. *Nano Lett.* **2003**, *3*, 1489.
(3) Berret, J.-F.; Schonbeck, N.; Gazeau, F.; El Kharrat, D.; Sandre, O.; Vacher, A.; Airiau, M. *J. Am. Chem. Soc.* **2006**, *128*, 1755.
(4) Sanson, C.; Diou, O.; Thévenot, J.; Ibarboure, E.; Soum, A.; Brûlet, A.; Miraux, S.; Thiaudière, E.; Tan, S.; Brisson, A.; Dupuis, V.; Sandre, O.; Lecommandoux, S. b. *ACS Nano* **2011**, *5*, 1122.
(5) Mueller, W.; Koynov, K.; Fischer, K.; Hartmann, S.; Pierrat, S.; Basché, T.; Maskos, M. *Macromolecules* **2008**, *42*, 357.
(6) Krack, M.; Hohenberg, H.; Kornowski, A.; Lindner, P.; Weller, H.; Förster, S. *J. Am. Chem. Soc.* **2008**, *130*, 7315.
(7) Binder, W. H.; Sachsenhofer, R.; Farnik, D.; Blaas, D. *Phys. Chem. Chem. Phys.* **2007**, *9*, 6435.
(8) Mai, Y.; Eisenberg, A. *J. Am. Chem. Soc.* **2010**, *132*, 10078.
(9) Kang, Y.; Taton, T. A. *Angew. Chem., Int. Ed.* **2005**, *44*, 409.
(10) Kim, B.-S.; Qiu, J.-M.; Wang, J.-P.; Taton, T. A. *Nano Lett.* **2005**, *5*, 1987.
(11) Hickey, R. J.; Haynes, A. S.; Kikkawa, J. M.; Park, S.-J. *J. Am. Chem. Soc.* **2011**, *133*, 1517.
(12) Sanchez-Gaytan, B. L.; Cui, W.; Kim, Y.; Mendez-Polanco, M. A.; Duncan, T. V.; Fryd, M.; Wayland, B. B.; Park, S.-J. *Angew. Chem., Int. Ed.* **2007**, *46*, 9235.
(13) Sanchez-Gaytan, B. L.; Li, S.; Kamps, A. C.; Hickey, R. J.; Clarke, N.; Fryd, M.; Wayland, B. B.; Park, S.-J. *J. Phys. Chem. C* **2011**, *115*, 7836.
(14) Kamps, A. C.; Sanchez-Gaytan, B. L.; Hickey, R. J.; Clarke, N.; Fryd, M.; Park, S.-J. *Langmuir* **2010**, *26*, 14345.
(15) Bockstaller, M. R.; Mickiewicz, R. A.; Thomas, E. L. *Adv. Mater.* **2005**, *17*, 1331.
(16) Chung, H.-J.; Kim, J.; Ohno, K.; Composto, R. J. *ACS Macro Lett.* **2011**, *1*, 252.
(17) Bockstaller, M. R.; Lapetnikov, Y.; Margel, S.; Thomas, E. L. *J. Am. Chem. Soc.* **2003**, *125*, 5276.
(18) Chiu, J. J.; Kim, B. J.; Kramer, E. J.; Pine, D. J. *J. Am. Chem. Soc.* **2005**, *127*, 5036.
(19) Li, Q.; He, J.; Glogowski, E.; Li, X.; Wang, J.; Emrick, T.; Russell, T. P. *Adv. Mater.* **2008**, *20*, 1462.
(20) Brust, M.; Walker, M.; Bethell, D.; Schiffrin, D. J.; Whyman, R. *J. Chem. Soc., Chem. Commun.* **1994**, 801.
(21) Chen, T.; Yang, M.; Wang, X.; Tan, L. H.; Chen, H. *J. Am. Chem. Soc.* **2008**, *130*, 11858.
(22) Kim, D. H.; Wei, A.; Won, Y.-Y. *ACS Appl. Mater. Interfaces* **2012**, *4*, 1872.
(23) Chung, H.-j.; Ohno, K.; Fukuda, T.; Composto, R. J. *Nano Lett.* **2005**, *5*, 1878.
(24) Pieranski, P. *Phys. Rev. Lett.* **1980**, *45*, 569.
(25) Israelachvili, J. N. *Intermolecular and Surface Forces*, 3rd ed.; Academic Press: Burlington, MA, 2011.
(26) Carré, A. *J. Adhes. Sci. Technol.* **2007**, *21*, 961.
(27) Kuna, J. J.; Voitchovsky, K.; Singh, C.; Jiang, H.; Mwenifumbo, S.; Ghorai, P. K.; Stevens, M. M.; Glotzer, S. C.; Stellacci, F. *Nat. Mater.* **2009**, *8*, 837.
(28) Laibinis, P. E.; Fox, M. A.; Folkers, J. P.; Whitesides, G. M. *Langmuir* **1991**, *7*, 3167.
(29) Zhang, L.; Eisenberg, A. *J. Am. Chem. Soc.* **1996**, *118*, 3168.
(30) Yu, Y.; Eisenberg, A. *J. Am. Chem. Soc.* **1997**, *119*, 8383.
(31) Kim, B. J.; Fredrickson, G. H.; Hawker, C. J.; Kramer, E. J. *Langmuir* **2007**, *23*, 7804.
(32) Hickey, R. J.; Sanchez-Gaytan, B. L.; Cui, W.; Composto, R. J.; Fryd, M.; Wayland, B. B.; Park, S.-J. *Small* **2010**, *6*, 48.
(33) Lin, Y.; Skaff, H.; Emrick, T.; Dinsmore, A. D.; Russell, T. P. *Science* **2003**, *299*, 226.